Phys Chem Minerals (2004) 31: 102–114
DOI 10.1007/s00269-003-0362-y

ORIGINAL PAPER

E. Schmidbauer · Th. Kunzmann

Electrical conductivity, thermopower and ^{57}Fe Mössbauer spectroscopy of aegirine ($NaFeSi_2O_6$)

Received: 22 January 2003 / Accepted: 26 August 2003

Abstract DC and AC electrical conductivities were measured on samples of two different crystals of the mineral aegirine ($NaFeSi_2O_6$) parallel (∥) and perpendicular (⊥) to the [001] direction of the clinopyroxene structure between ~200 and ~600 K. Impedance spectroscopy was applied (20 Hz–1 MHz) and the bulk DC conductivity σ_{DC} was determined by extrapolating AC data to zero frequency. In both directions, the log $\sigma_{DC} - 1/T$ curves bend slightly. In the high- and low-temperature limits, differential activation energies were derived for measurements ∥ [001] of E_A ~0.45 and ~0.35 eV, respectively, and the numbers ⊥ [001] are very similar. The value of σ_{DC} ∥ [001] with σ_{DC}(300 K) $\sim 2.0 \times 10^{-6}$ $\Omega^{-1}cm^{-1}$ is by a factor of 2–10 above that measured ⊥ [001], depending on temperature, which means anisotropic charge transport. Below ~350 K, the AC conductivity $\sigma'(\omega)$ ($\omega/2\pi$ = frequency) is enhanced relative to σ_{DC} for both directions with an increasing difference for rising frequencies on lowering the temperature. An approximate power law for $\sigma'(\omega)$ is noted at higher frequencies and low temperatures with $\sigma'(\omega) \propto \omega^s$, which is frequently observed on amorphous and disordered semiconductors. Scaling of $\sigma'(\omega)$ data is possible with reference to σ_{DC}, which results in a quasi-universal curve for different temperatures. An attempt was made to discuss DC and AC results in the light of theoretical models of hopping charge transport and of a possible $Fe^{2+} \rightarrow Fe^{3+}$ electron hopping mechanism. The thermopower Θ (Seebeck effect) in the temperature range ~360 K < T < ~770 K is negative in both directions. There is a linear $\Theta - 1/T$ relationship above ~400 K with activation energy E_Θ ~0.030 eV ∥ [001] and 0.070 eV ⊥ [001]. ^{57}Fe Mössbauer spectroscopy was applied to detect Fe^{2+} in addition to the dominating concentration of Fe^{3+}.

Keywords Electrical conductivity · Impedance spectroscopy · Thermopower · ^{57}Fe Mössbauer spectroscopy · Aegirine

E. Schmidbauer (✉)
Department für Geo- und Umweltwissenschaften,
Sektion Geopysik, der Universität München,
Theresienstr 41, 80333 München, Germany
e-mail: schmidba@geophysik.uni-muenchen.de
Fax: 89-2180-4205
Tel.: 89-2180-4212

Th. Kunzmann
Department für Geo- und Umweltwissenschaften,
Sektion Mineralogie,
Petrologie und Geochemie,
der Universität München,
Theresienstr.41,
80333 München, Germany

Introduction

Natural silicates belong in general to the group of electrical insulators, hence, the electrical conductivity is comparatively low. The highest conductivity was as a rule observed on Fe-rich silicates, which was found by comparing experimental conductivity results of a large number of silicates (Parkhomenko 1982; Schmidbauer et al. 2000). Obviously, the presence of Fe cations frequently enhances electrical charge transport. A detailed investigation of the related charge-transfer mechanism, however, is still missing. In this communication we present data on the electrical conductivity of an Fe-rich clinopyroxene, aegirine (ideal composition $NaFe^{3+}Si_2O_6$).

The general pyroxene structure consists of infinite chains of SiO_3 groups extending along the [001] direction, linked by cations (Fig. 1). M1 octahedra form zigzag chains along [001]; an M1 octahedron shares edges with two other M1 octahedra and three M2 polyhedra. All six corners of M1 octahedra are shared with T tetrahedra. In natural pyroxenes, occasionally exsolution intergrowth and chemical inhomogeneities are observed (Buseck et al. 1980; Cameron and Papike 1981). In natural aegirine, Na^+ cations are in some instances replaced by Ca^{2+}, which is accompagnied by incorporation of Fe^{2+}. This fact may give rise to electron hopping $Fe^{2+} \rightarrow Fe^{3+}$ between localized levels. Whether long

range charge transport can take place depends evidently on the concentration of Ca^{2+}. In this case such a mechanism can dominate electrical conduction. We studied the electrical conductivity of natural monocrystalline aegirine samples with the aim of elucidating whether the presence of Fe is in fact an important factor in electrical charge transport. Impedance spectroscopy was applied (20 Hz–1 MHz) in order to be able to distinguish bulk charge transport from charge transfer processes at the interface sample–electrode. Furthermore, the thermopower (Seebeck effect) of aegirine samples was determined, which gives further independent information on the charge transport mechanism.

Typical literature values of the electrical conductivity σ for Fe-rich clinopyroxenes are: aegirine and hedenbergite ($CaFeSi_2O_6$) with σ (573 K) $\sim 10^{-4}$ $\Omega^{-1}cm^{-1}$ at atmospheric pressure (Parkhomenko and Mkrtchyan 1974; Parkhomenko 1982). Results for Fe-poor natural pyroxenes are: jadeite ($NaAlSi_2O_6$) σ (573 K) $\sim 2 \times 10^{-7}$ $\Omega^{-1}cm^{-1}$, spodumene ($LiAlSi_2O_6$) σ (573 K) $\sim 10^{-9}$ $\Omega^{-1}cm^{-1}$, diopside ($CaMgSi_2O_6$) σ (573 K) $\sim 10^{-10}$ Ω^{-1} cm^{-1} (ideal compositions are given in brackets). In all cases no directional dependencies were reported. Thus, Fe- bearing clinopyroxenes appear to exhibit higher conductivity. On the other hand, from conductivity measurements on a series of orthopyroxene samples in the high-temperature region $>$ 1000 K it was concluded that the Fe concentration cannot be the major determining factor affecting conductivity (Huebner et al. 1979); the authors suspected that Al and Cr may also contribute to increased conductivity.

Samples and experimental procedure

Samples

Samples were cut from two natural aegirine single crystals using a wire saw (large aegirine LA: $\sim$60 mm long with square cross-section 12×12 mm^2, small aegirine SM : $\sim$25 mm long with square cross-section 5×5 mm^2), both from Mt. Malosa (Malawi, Africa). The chemical composition, as found by electron microprobe (CAMECA SX50) analysis, is as follows:

$$\text{aegirine LA}\{Na_{0.86}Ca_{0.09}\}\left((Fe^{2+}, Fe^{3+})_{0.93}Ti_{0.03}Mn_{0.03}\right)[Si_{2.000}]O_6, \quad \text{including } V_{0.002}, Mg_{0.006}, Al_{0.007}$$

$$\text{aegirine SM}\{Na_{0.99}Ca_{0.01}\}\left((Fe^{2+}, Fe^{3+})_{1.00}\right)[Si_{2.000}]O_6, \quad \text{including } V_{0.002}\ ,$$

where brackets { } denote M2, ( ) M1 and [ ] T sites. Lattice parameters for synthetic aegirine are $a = 9.658$ Å, $b = 8.795$ Å, $c = 5.294$ Å and ß = 107.42° (Nolan 1969). We found for aegirine LA: $a = 9.664$ Å, $b = 8.813$ Å, $c = 5.277$ Å, ß = 107.61° and for aegirine SM: $a = 9.658$ Å, $b = 8.811$ Å, $c = 5.285$ Å and ß = 107.62° (Philips diffractometer PW1830, graphite monochromator, Cu–K_α-radiation). ^{57}Fe Mössbauer data were utilized to discriminate between Fe^{2+} and Fe^{3+}, as will be described below.

In the samples of aegirine LA used for electrical measurements light microscopic analyses of polished surfaces (001 plane) revealed many round and elongated holes ($\sim$5 µm) of the order of $\sim$100 mm^{-2} and, in addition, a few larger ones of dimensions of $\sim$50–100 µm. All holes were as a rule well separated from each other. We suspect that the holes might contain gas inclusions. In samples of aegirine SM a perfect surface was noted without holes and other defects.

^{57}Fe Mössbauer spectra

From Mössbauer spectra recorded at two temperatures (Fig. 2), concentration ratios $[Fe^{2+}]/[Fe^{3+}]$ were determined which may be of interest for electrical conduction by electron hopping $Fe^{2+} \rightarrow Fe^{3+}$. The 85 K spectrum of aegirine LA shows a central doublet, due to Fe^{3+}, and a small peak in the positive velocity range at $\sim +$ 2.8 mm^{-1}/s that arises doubtless from Fe^{2+} cations. A fit of two symmetrical doublets to the pattern results in an Fe^{2+} doublet with a too large line width $B = 0.39$ mm^{-1}/s (FWHM) which means that the doublet is a superposition of at least two doublets. For such a fit, however, constraints have to be imposed in order to obtain reasonable Mössbauer parameters. In the literature, a two-Fe^{2+} doublet fit was made to a liquid nitrogen temperature spectrum of a synthetic solid solution of 20% hedenbergite ($CaFeSi_2O_6$) and 80% aegirine (hed20/aeg80) (Dollase and Gustafson 1982); this spectrum resembles our spectrum qualitatively. The authors also used a three-Fe^{2+} doublet fit, imposing

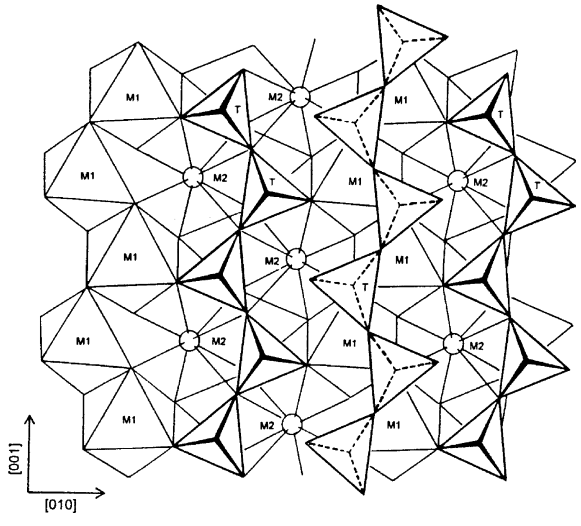

Fig. 1 Characteristic features of the clinopyroxene structure. (After Cameron and Papike 1981)

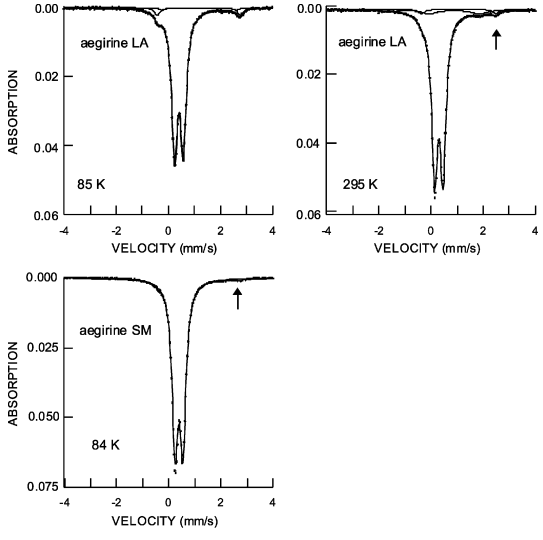

Fig. 2 ^{57}Fe Mössbauer spectra of aegirine LA and SM

constraints to the fit parameters, and found equality to a two-Fe^{2+} doublet fit; they did this with the argument that such a fit may be coupled to the number of different near-neighbour environments affected in particular by the arrangement of Ca and Na on M2 sites, which can be assumed to be grouped into three classes. Three Fe^{2+} doublets were also used for a fit to an 80 K spectrum of synthetic hed10/aeg90 (Redhammer et al. 2000).

For the 85 K spectrum of aegirine LA, we constrained the linewidth B for both Fe^{2+} doublets to $B = 0.27$ mm s^{-1} and both isomer shift IS values were kept equal, while all other fitted parameters were freed. Mössbauer parameters are presented in Table 1. For Fe^{3+} on M1 sites, the comparatively small quadrupole splitting $QS = 0.32$ mm s^{-1} and line width $B = 0.28$ mm s^{-1} point to rather regular M1 octahedra and, in addition, to a rather homogeneous near-neighbour environment; in this context one has to bear in mind that as impurities there are a notable concentration of $Ca_{0.09}$ apfu on M2 sites and $Mn_{0.03}$ and $Ti_{0.03}$ apfu on M1 sites. The Fe^{3+} parameters agree with literature data (Dollase and Gustafson 1982; Amthauer and Rossman 1984; Ballet et al. 1989; Redhammer et al. 2000). From area ratios, the ratio $[\Sigma Fe^{2+}]/[\Sigma Fe] = 0.078$ was derived (suggesting f-factors to be identical for all Fe ions). For the 295 K spectrum, the high-velocity peak of Fe^{2+} is rather small, as visible from Fig. 2. It appears that in fact two peaks may exist. We fitted the pattern as the 85 K spectrum. Mössbauer parameters are listed in Table 1. It turned out that for one Fe^{2+} doublet the line width $B = 0.76$ mm s^{-1} is excessively broad. This may be the consequence of the fact that a superposed largely continuous absorption exists between the outermost high-velocity Fe^{2+} peak and the high-velocity peak of the Fe^{3+} doublet. Such an absorption can be the result of electron hopping $Fe^{2+} \rightarrow Fe^{3+}$ with a hopping frequency close to the critical Mössbauer frequency of $\sim 10^8$ s^{-1}, which may result in relaxation spectra.

From the 84 K spectrum of aegirine SM (Fig. 2), an indication of a very small concentration of Fe^{2+} is noted, marked by an arrow in the positive velocity range. No such irregularity could be observed from the 295 K pattern. The 84 K pattern was fitted using one doublet (Table 1).

Experimental procedure

DC and AC electrical conductivity measurements were performed with the help of an HP 8294 A precision LCR meter in the frequency range 20 Hz–1 MHz applying a four terminal cable method. The measured quantities are given with an error $< 0.1\%$. DC data were obtained by extrapolating AC impedance results to zero frequency. Measurements were performed between $\sim$200 and $\sim$800 K, using a minicryostat below $\sim$295 K and a water-cooled minifurnace above. Sample temperatures were monitored by NiCr–Ni thermocouples for temperatures below and above 295 K, respectively. Temperatures were kept constant to $\pm$ 0.2 K with the help of temperature controllers. Conductivity measurements were performed fully automatically. All measurements above 295 K were conducted in N_2 gas atmosphere.

For thermopower measurements, the samples were clamped between circular Pt plate electrodes (diameter $\sim$6 mm) and Pt leads were applied. One electrode was heated with a microheater to generate a temperature difference ΔT between both sample faces, which produces a sample thermovoltage U_{th}. Electrode temperatures were measured with two thermocouples attached to the Pt plates. The whole sample cell was inserted in a tube furnace in order to vary the average sample temperature up to $\sim$800 K. All voltages were measured with HP34420 A nanovoltmeters (input resistance $> 10^{10}$ Ω) with an error $< 1\%$. Temperatures were measured with an accuracy of $\pm$ 0.1 K. For each measurement, five values of ΔT in the range 0–4 K were generated and the thermopower Θ ($\Theta = U_{th}/\Delta T$) was determined from the slope U_{th} versus ΔT in order to eliminate the effect of disturbing offset voltages. Absolute Θ values are given considering experimental data of the thermopower of Pt (Moore and Graves 1973). All measurements were performed fully automatically using a PC program.

Sample parallelepipeds were prepared, ground and polished (Struers no. 1200); typical sample dimensions were $4 \times 4 \times 2.5$ mm^3. For low-temperature measurements, the sample dimension between the electrodes was reduced to $\sim$1 mm in order to keep the impedance small. After contacting two opposite faces of a sample with Pt paint (followed by preheating to $\sim$350 K in air), it was spring-loaded between the electrodes (Ag paint or In/Ga (7:3) as contacting material at not too high temperatures proved to be less favourable). For measurements of the dielectric permittivity, a circular sample with the diameter of the electrodes was used.

Results

DC conductivity

Impedance spectroscopy was utilized plotting the real part of the impedance, Z', against the imaginary part, Z'', on the complex impedance plane for frequencies in the range 20 Hz–1 MHz. Figure 3a,b shows typical results for aegirine SM at various temperatures; parameter is the frequency. In Fig. 3a, one semicircular arc can be seen at 231 K for measurements parallel ($\|$) to the [001] direction and the onset to a second one at the lowest frequencies. At a higher temperature of 288 K, the second huge arc is more clearly visible. Our frequency window does not allow us to observe the whole arc 2. The arc 1 next to the coordinate origin arises from bulk charge-transport processes. This follows from the low capacitance related to this arc. The arc 2, of which only the high-frequency flank is observed, is in principle due either to electronic processes at lattice defects or to the

Table 1 Fitted ^{57}Fe Mössbauer parameters for the aegirine spectra of Fig. 2; QS quadrupole splitting, IS isomer shift (with regard to metallic Fe); B line width; F area fraction of ΣFe^{2+}

	T(K)	QS(mm s^{-1})	IS(mm s^{-1})	B(mm s^{-1})	F
Aegirine LA					
Fe^{3+}	295	0.32	0.43	0.28	–
Fe^{2+} 1	295	2.81	1.18	1.18	0.26
Fe^{2+} 2	295	1.93	1.02	0.76	
Fe^{3+}	85	0.34	0.53	0.28	
Fe^{2+} 1	85	3.16	1.28	0.27	0.078
Fe^{2+} 2	85	2.83	1.28	0.27	
Aegirine SM					
Fe^{3+}	84	0.30	0.52	0.27	
Fe^{2+}	84				< 0.03

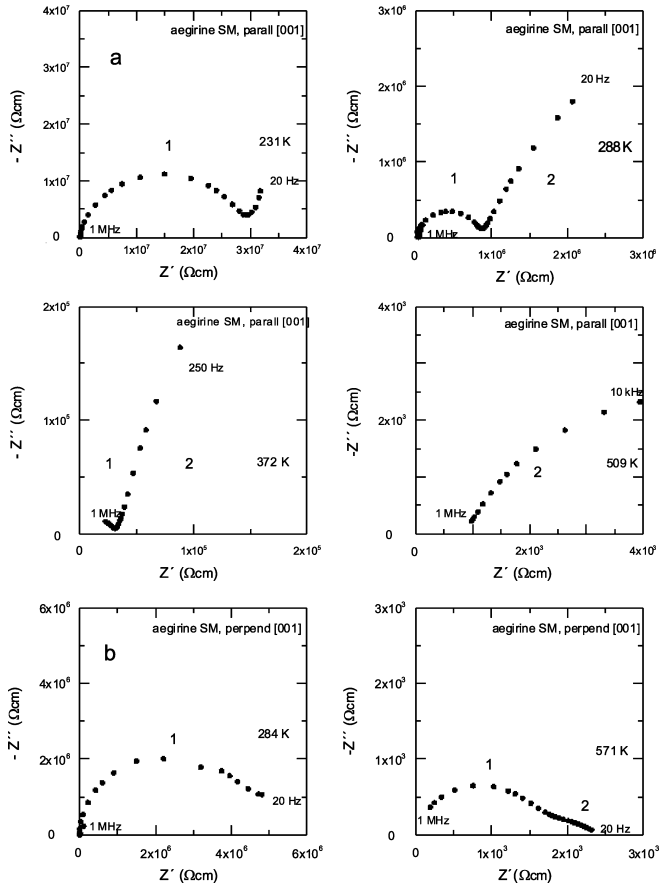

Fig. 3 a, b Real part of the impedance, Z', against the imaginary part, Z'', on the complex impedance plane for aegirine SM at different temperatures; parameter is the frequency. Measurements: **a** $\parallel$ [001], **b** $\perp$ [001]

interface sample–electrode. It turned out that the arcs 2, measured $\parallel$ [001], were much larger than those recorded perpendicular ($\perp$) to [001] at the same temperature. The DC resistivity could be determined by extrapolating arc 1 next to the origin to its low-frequency intersection with the Z' axis. The minimum frequency of 20 Hz is not sufficiently low to detect the whole arc 2. We made a check to test whether arc 2 is due to interfacial processes for measurements $\parallel$ [001] by cutting a sample to half its original thickness. This procedure should diminish arc 1 by a factor of 2 and leave arc 2 unchanged. Indeed, this effect was observed. We could not detect a large difference in the magnitude of arc 2, when 1 V or 20 mV was applied at the sample electrodes; a variation with voltage is in general established in the presence of a Schottky barrier at the interface sample–electrode.

By increasing the temperature, a rising part of arc 2 can be observed in the frequency window 20 Hz–1 MHz at the cost of arc 1 until at high temperatures only arc 2 is visible (Fig. 3a). To measure arc 1, frequencies in excess of 1 MHz are required. In this case, we determined the bulk DC resistivity, due to arc 1, from data of arc 2 extrapolating to infinite frequency and taking the intersection point with the Z' axis. For a series of temperatures, we made fits to arc 1 using the method of Tsai and Whitmore (1982). It turned out, however, that a direct reading from the plots of the arcs by extrapolation is sufficient in most cases when the maximum is determined. At higher temperatures, we estimate the error of measurement to range up to 10–15% that can be tolerated because the DC resistivity is varying orders of magnitude with temperature.

Figure 3b displays analogous impedance data taken on aegirine SM $\perp$ [001]. A situation exists very similar as for measurements $\parallel$ [001]. At 284 K, arc 1 and the transition to arc 2 are seen, while two semicircular arcs can be detected at higher temperatures. The low-frequency part of arc 1 can be clearly observed up to the maximum applied temperature.

DC conductivity $\parallel$ [001]

For aegirine SM and LA, the temperature variation of the bulk DC conductivity $\sigma_{DC} \parallel$ [001] is presented in Fig. 4a for temperatures between ~220 and 600 K. The DC curves represent a superposition of data points during several measurement runs on heating and cooling. No notable variation could be detected between these datasets up to the maximum temperature applied. Obviously, by the heating procedure no alteration of the bulk charge-transport processes takes place. Measurements at $T \geq 600$ K were excluded because of the increasing error during extrapolation of σ_{DC} from the relevant arc 2. Slightly bent curves are observed, hence no strictly activated behaviour is found. A closer inspection shows that interpretation of a whole curve in terms of two straight lines with a break is not adequate. However, we approximate each curve by straight lines in the limit of high and low temperatures which allows differential activation energies to be deducted. We tentatively apply the model of a hopping charge transport by small polarons between localized states of nearest-neighbours. Polar lattices such as oxides exhibit in general strong electron–lattice interaction which gives rise to a lattice distortion in the environment of a hopping electron. The electron plus the induced lattice distortion, termed polaron, has lower energy than the undistorted crystal. When the polaron cloud is restricted to a radius smaller than the nearest-neighbour hopping separation, the polaron is said to be small, while for a large polaron this region is more extended (Austin and Mott 1969). For hopping of polarons between localized states, theoretical models treat two different kinds of hopping: (1) phonon-assisted over barrier hopping and (2) phonon-assisted quantum-mechanical tunnelling through energy barriers. For the latter kind of hopping of small polarons, in the non-adiabatic approximation at temperatures $T > \Theta_D/2$ (Θ_D = Debye temperature), the relation

$$\sigma_{DC} = (e^2 v_0 / R k_B T) c(1-c) \exp(-2\alpha R) \exp(-W/k_B T) \quad (1)$$

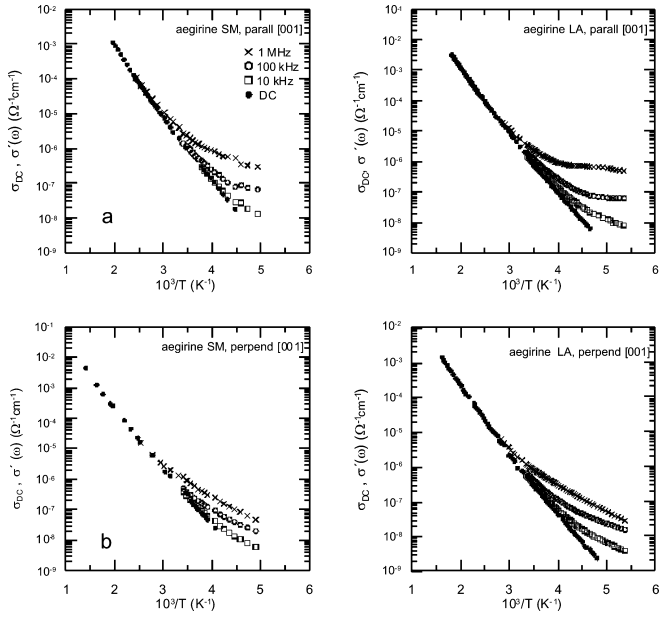

Fig. 4 **a** Temperature dependence of the extrapolated DC conductivity σ_{DC} and of AC conductivity $\sigma'(\omega)$ (1 MHz, 100 kHz, 10 kHz) recorded $\parallel$ [001] for aegirine SM and LA; the same symbols are used for all plots: ● DC, × 1 MHz, ○ 100 kHz, □ 10 kHz. **4b** As in **a**, recorded $\perp$ [001] for aegirine SM and LA

was derived (Austin and Mott 1969); e is the electronic charge, ν_0 is a mean phonon frequency related to Θ_D by $h\nu_0 = k_B\Theta_D$ where h is Planck's and k_B Boltzmann's constant; R is the hopping distance to the nearest neighbour, c is the fraction of available hopping sites occupied by charge carriers, α is the s-type wave function decay parameter at a site (α^{-1} = localization length of hopping electrons near the Fermi level), W is the hopping activation energy at high temperatures which consists of two energies $W = E_H + E_D/2$; E_H is the hopping activation energy of polarons as a consequence of polarization and E_D is the spread of energy states due to random fields. The term exp(-2αR) describes the overlap of the wave functions of neighbouring hopping sites.

From the plot $\log(T\sigma_{DC})$ versus $1/T$ (replotting of Fig. 4a) it follows in the high-T limit for aegirine SM from a least-squares fit an activation energy of $W = 0.42$ eV and for aegirine LA it results in $W = 0.47$ eV; in the low temperature ranges we deduce for both aegirines $W = 0.33$ and 0.37, respectively; these values are associated with an estimated error of $\sim \pm$ 0.02 eV. No notable differences are in fact noted for both aegirines, although aegirine LA contains more impurities (also more Fe^{2+}) and hence, the disorder is enhanced relative to aegirine SM. At higher temperatures, σ_{DC} of aegirine LA is by a factor of about 3–4 above the data for aegirine SM. We suppose charge transport to be effected primarily by $Fe^{2+} \rightarrow Fe^{3+}$ electron hopping and suggest tentatively that all Fe ions take part in conduction. For aegirine LA we estimate for the concentration c of donors, represented by Fe^{2+}, $c = 0.078$ (from Mössbauer data of Table 1). Using as phonon frequency $\nu_0 = 1 \times 10^{13}$ s^{-1} and as hopping distance between nearest-neighbour Fe^{2+} and Fe^{3+} on M1 sites $R = 3.19$ Å (Ballet et al. 1989) we infer, applying Eq. (1), $\alpha^{-1} \sim 40$ Å. This magnitude is far beyond the range of $\alpha^{-1} \leq R$ expected for small polarons. One has to bear in mind that the applied value of ν_0 is an estimate commonly used in the literature. For aegirine SM it results with $c \sim 0.02$ a value of $\alpha^{-1} \sim 10$ Å. In both cases a localization length for α^{-1} follows, rather typical for intermediate polarons (between small and large polarons in extension). Using in both cases a higher ν_0 value depresses α^{-1} to lengths which are of the expected order of magnitude for small polarons. Although the estimations are no strict proof for the applied model they show that (1) the assumption of $Fe^{2+} \rightarrow Fe^{3+}$ hopping makes sense and (2) application of Eq. (1) of the model of small polaron tunnelling leads to a reasonable order of magnitude for α^{-1}.

We also made an attempt to verify a formula derived for the DC conductivity of small polarons in the high- and low-temperature regions (Schnakenberg 1968). This theory is based on the concept that the hopping activation energy is composed of a contribution by E_H and one due to E_D. In the high-temperature regions hopping is effected by multiple optical phonon processes while at the lowest temperatures acoustic single-phonon processes are dominating. According to the notation by Mott (1968) it is:

$$\sigma_{DC} = (C_S/T)\exp(-2\alpha R)\exp(-E_D/2k_BT) \times \exp[(-4E_H/h\nu_0)\tanh(h\nu_0/4k_BT)] \quad , \qquad (2)$$

where the parameters were defined above and C_S is a constant. We tried to approximate our σ_{DC} data for aegirine LA $\parallel$ [001] in Fig. 5a by Eq. (2), although only a weak bending of the curve is available owing to the lack of data in the low-temperature region due to a too high resistance, as mentioned. With quite reasonable parameters, $E_H = 0.43$ eV, $E_D = 0.094$ eV, $\nu_0 = 1.1 \times 10^{-13}$ s^{-1} and a constant C_S, we obtained the satisfying approximation presented in Fig. 5a ($\chi^2 \sim 2$), taking the term exp (-2αR) to the constant (without trying to determine the quantity αR). In addition to activation energy quite similar to that obtained from Eq. (1), information is gained of the disorder energy E_D, with the average $\langle E_D \rangle \sim 0.047$ eV. Both values are comparable to those observed on amorphous and disordered semiconductors, gained from analogous weakly bent curves and using a formula differing slightly from Eq. (2), such as V-phosphate glasses (Sayer et al. 1971), V_2O_5 gels (Sanchez et al. 1982), Bi–V oxide glasses (Gosh 1990), Te–Mo oxide glasses (Gosh 1992) and Sr–V oxide glasses (Sen and Gosh 1999). We estimate roughly $\Theta_D = h\nu_0/k_B \sim 430$ K, which is consistent with the fact that the expected strong bending of the σ_{DC} curve as expected at $\Theta_D/4 \sim 110$ K was not accessible to our measurements.

We also tried to analyze σ_{DC} data below about 300 K using plots $\log \sigma_{DC} - T^{-1/4}$ or $-T^{-1/2}$. Both relationships should give straight lines in the case of variable range

hopping (VRH) for certain charge-hopping models. VRH is a charge transport process at low temperatures, where hopping (tunnelling) to more distant localized sites with low-energy barriers is favoured relative to nearest-neighbour hopping with higher barriers. The first relation is obeyed in the case of three-dimensional (3 D) hopping conduction (Mott and Davis 1979), the second in the presence of electron–electron interaction (Efros and Shklovskii 1975) and in the case of one-dimensional (1 D) hopping (Bloch et al. 1972; Brenig et al. 1973; Shante et al. 1973; Serota et al. 1986; Hunt 1991a,b; Bleibaum et al. 1996). For the description of 1 D transport, apart from Bleibaum et al. (1996), charge transfer is presumed to occur along chains of finite lengths and packed parallel in bundles. Furthermore, interchain hopping is allowed to a variable degree, with a hopping rate lower than parallel to the chain. If interchain charge transfer is enhanced, in fact a 3 D hopping model may be applicable. Formulae were derived for the conductivity σ_{DC} along the chains with $\sigma_{DC} \propto \exp(-(T_0/T)^{1/2})$ where T_0 differs for the various authors. We use the expression by Shante et al. (1973), which does not contain the chain lengths, in contrast to that of the other authors, of $T_0 = 4\alpha/(N(E_F)k_B)$, where α^{-1} is the localization length of a hopping charge, $N(E_F)$ is the density of states per eV and cm of the chains. For aegirine LA and SM, $T^{-1/2}$ plots give straight lines below ~360 K, as shown for aegirine LA in Fig. 5b. From a fit of the data we infer $T_0 = 2.9 \times 10^5$ K for aegirine LA and a very similar value for aegirine SM. It follows that $N(E_F)\,\alpha^{-1} \sim 0.16\ eV^{-1}$. For both aegirines, the $T^{-1/4}$ relation describes the data less satisfactorily. For quite a number of amorphous and disordered semiconductors a $T^{-1/4}$ dependence was established in certain temperature ranges, while only a few $T^{-1/2}$ dependences were reported (Wang et al. 1991, Capaccioli et al. 1998; Koscielska et al. 1999).

DC conductivity ⊥ [001]

It appears from Fig. 4b that there is hardly any qualitative difference to measurements ∥ [001]. Differential E_A values in the high- and low-T limits are $E_A = 0.45$ eV and 0.33 eV, respectively. Since no hopping distance R is immediately evident, we did not apply the full Eq. (1). All σ_{DC} values recorded ∥ [001] are a factor of ~2–10 above those ⊥ [001], depending on temperature. Hence, the charge transport in our aegirine sample is evidently anisotropic. From the otherwise very similar behaviour of σ_{DC} ∥ and ⊥ [001] it seems as if in principle only a variation in the concentration of charge carriers exists in both cases. We found that for our parallelepiped sample both possible directions ⊥ [001] show hardly any difference in magnitude of σ_{DC} at room temperature. For this reason we measured only σ_{DC} ⊥ [001] for one direction, whose exact structural orientation remains unknown. An attempt to use the above $T^{-1/4}$ or $T^{-1/2}$ laws did not result in adequate straight lines.

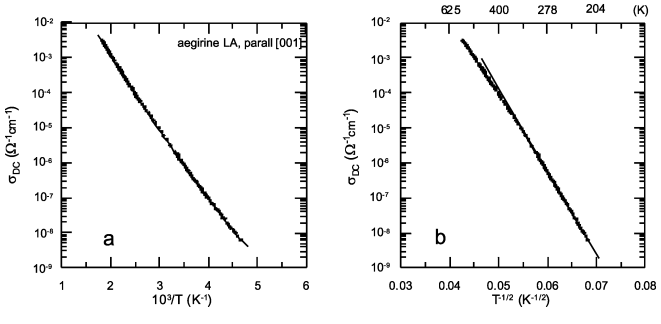

Fig. 5 **a** Temperature variation of σ_{DC} ∥ [001] for aegirine LA and approximation of the data by a formula of Schnakenberg(1968) (*solid line*). **b** Presentation of data in a $T^{-1/2}$ plot and fit at lower temperatures (*solid line*)

AC conductivity

In Fig. 4a,b, the AC conductivity $\sigma'(\omega)$ ($\omega = 2\pi\nu$, with ν = frequency) is presented for measurements at 10 kHz, 100 kHz and 1 MHz. At low temperatures, there is a considerable dispersion. Because of the enhanced $\sigma'(\omega)$ relative to σ_{DC}, data could be measured to lower temperatures. As is seen from Fig. 4a for both aegirines SM and LA, the $\sigma'(\omega)$ curves merge into the σ_{DC} curve at different temperatures. At 1 MHz, for example, it seems to occur at ~400 K, and this temperature shifts to lower temperatures with decreasing frequencies. For 1 MHz and 100 kHz at low temperatures, the differential activation energies are tending towards zero. A very similar behaviour of $\sigma'(\omega)$ is observed for data taken ⊥ [001] (Fig. 4b).

Frequency dependence of AC conductivity

The frequency dependence of $\sigma'(\omega)$ in a log–log presentation is shown in Fig. 6 for measurements ∥ and ⊥ [001] for aegirine LA at different temperatures. For each dataset, there appears to be the onset to a rather linear relation in the high-frequency region, which is shifting with temperature. At frequencies >> 1 MHz, the curves are expected to tend to saturation values. The critical frequency where $\sigma'(\omega)$ starts to rise from σ_{DC} cannot be traced for all temperatures towards low frequencies, because in this frequency region data points are related in part to arc 2 (Fig. 3) in the Z'–Z'' presentation of data. This effect means a bending downwards of curves in this frequency regime. All related data points lie on arc 2 of Fig. 3, which stems from electrode contact layers; hence, these points are irrelevant for bulk data analysis. For data recorded ∥ [001] no indication of an onset towards saturation is visible, but such an effect is obvious ⊥ [001] for $T \geq 231$ K, although saturation is expected for much higher frequences. Saturation at frequences of the order of ~1 MHz was rarely established, such as for $La_2NiO_{4+\delta}$ in the basal plane (Jhans et al. 1996). An approximately linear relationship in the case of hopping charge transport was established in many

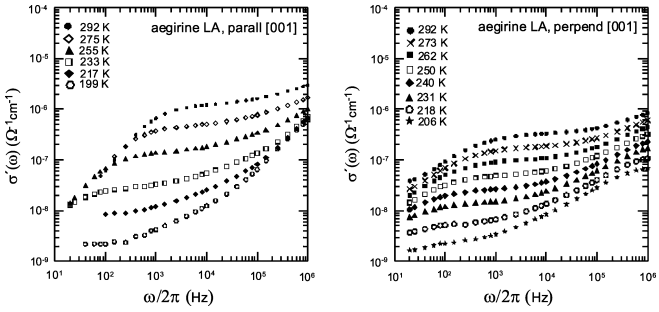

Fig. 6a,b Frequency dependence of $\sigma'(\omega)$ for aegirine LA in a log–log presentation; parameter is the temperature. **a** ∥ [001], **b** ⊥ [001]

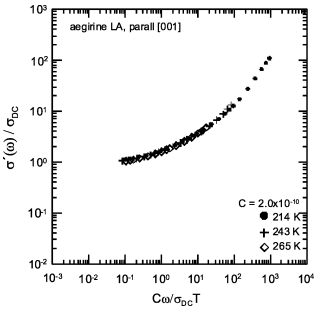

Fig. 7 Scaling of $\sigma'(\omega)$ with σ_{DC} for aegirine LA measured ∥ [001] according to a method proposed by Summerfield (1985) *C* represents a constant

amorphous and disordered semiconductors (reviews (Long 1982, 1991; Elliott 1987; Van Staveren et al. 1990)). The data can be described by the relation:

$$\sigma'(\omega) \propto \omega^{s(T)} \quad , \tag{3}$$

which holds with a temperature-dependent exponent *s*. Frequently, the exponent *s* is weakly varying with frequency in certain frequency ranges.

Scaling law of AC conductivity

In the so-called extended-pair approximation (EPA) (Summerfield 1985), which considers hopping round a pair of states in an averaged way, theory predicts a scaling law which allows the normalized $\sigma'(\omega)$ data to be presented in the form of some kind of quasi-universal curve

$$\sigma'(\omega, T)/\sigma_{DC}(T) = F(\omega*) \quad , \tag{4}$$

with $\omega^* = A^* e^2 \ \alpha\omega/(k_B T \ \sigma_{DC}(T))$, where F means a function, A* is a material-dependent constant. Summerfield proposed as a suitable function $F(x) = 1 + x^{0.725}$. This relation is based on the concept that AC and DC conductivity are due to the same charge–transport mechanism, i.e. it can serve as proof of our assumption that for the supposed hopping mechanism $\sigma_{DC} = \lim\omega\to 0 \ \sigma'(\omega)$. For measurements of aegirine LA ∥ [001], results are presented in Fig. 7 in the log–log presentation $\sigma'(\omega)/\sigma_{DC}$ versus $C\omega/\sigma_{DC}T$ for various temperatures, with C a constant.

AC losses

AC losses are the energy dissipated in the form of heat if an AC field is applied. In a dielectric, they are to be expected when permanent dipoles are present. Losses are also due to electron hopping processes between pairs of localized sites; theoretically, these hopping electrons can be treated as rotating dipoles. In order to discuss the related losses appropriately, it is useful to introduce the concept of the complex AC conductivity $\sigma^*(\omega) = \sigma'(\omega) + i\ \sigma''(\omega)$. Workers studying electric properties of dielectrics are accustomed to analyze their results in the language of the complex dielectric function $\varepsilon^*(\omega) = \varepsilon'(\omega) - i\ \varepsilon''(\omega)$, where $\varepsilon'(\omega)$ is the frequency-dependent relative dielectric permittivity (dielectric constant) and $\varepsilon''(\omega)$ is referred to as the dielectric loss. Both sets of quantities are interrelated by: $\sigma'(\omega) = \varepsilon_0\omega\varepsilon''(\omega)$, $\sigma''(\omega) = \varepsilon_0\omega\varepsilon'(\omega)$ (ε_0 is the vacuum permittivity) (Elliott 1987; Van Staveren et al. 1990), hence, the loss $\varepsilon''(\omega) = \sigma'(\omega)/\varepsilon_0\omega$. From the frequency dependence of $\varepsilon''(\omega)$ for aegirine SM measured ∥ [001] in a log–log presentation in Fig. 8a, no loss peak is observed between 20 Hz and 1 MHz.

In the literature, the presentation of the loss in a normalized form was proposed within the framework of the EPA approximation, given by the function $F_{NL}(\omega) = (\sigma'(\omega) - \sigma_{DC})/\ \sigma_{DC}\omega^*$ versus ω^*, where the normalized frequency ω^* was defined above (Summerfield 1985; Long et al. 1988; Dyre 1988a; Long 1991). It represents the AC response without percolating hopping processes. Figure. 8b displays $F_{NL}(\omega)$ versus ω^* for aegirine SM, measured ∥ [001], in a log–log presentation. Indeed also here a nearly quasi-universal curve appears to exist, because the curves superpose for three temperatures. Loss peaks appear to exist which were not established in the usual presentation $\varepsilon''(\omega)$ vs. ω; but they also appear if $\varepsilon''(\omega) = (\sigma'(\omega) - \sigma_{DC})/\ \varepsilon_0\omega$ is plotted versus ω without normalization. It should be noted that these considerations have to refer to frequencies related to arc 1 in the Z'–Z'' presentation of data in Fig. 3; all frequences reflecting arc 2 (due probably to interfacial electrode contact effects) have to be excluded. We suspect that our peak frequences ω^*_m could possibly be

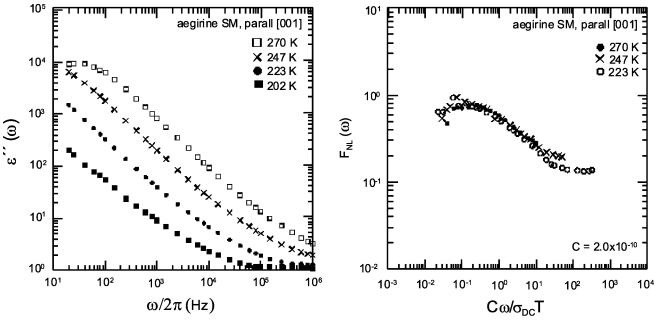

Fig. 8a,b Dielectric loss $\varepsilon''(\omega)$ as a function of frequency for aegirine SM measured ∥ [001] in a log–log presentation for some temperatures

related in part or completely to interfacial processes reflecting properties of arc 2 in Fig. 3.

Dielectric permittivity

The dielectric permittivity is also a parameter which shows typical characteristics of electronic and ionic processes in a compound. For aegirine LA ∥ [001], Fig. 9a depicts the temperature variation of the relative dielectric permittivity $\varepsilon'(\omega)$ for four frequencies. At higher temperatures, a considerable dispersion is evident, while it is weak at low temperatures. In Fig. 9b, the frequency dependence of $\varepsilon'(\omega)$ is presented at several temperatures. In this data presentation, the tendency towards very similar values at higher frequencies is quantitatively seen, and can be considered as high-frequency values; at 1 MHz, a weak variation with temperature can be recognized.

Thermopower Θ

The temperature dependence of the absolute thermopower Θ is displayed in Fig. 10 for aegirine SM, measured ∥ and ⊥ [001] and for aegirine LA ∥ [001]. Θ is negative for both directions. Data taken ∥ [001] on

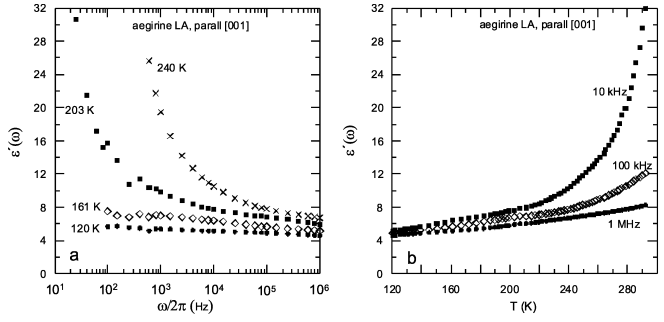

Fig. 9a,b Relative dielectric permittivity $\varepsilon'(\omega)$ of aegirine LA as a function of frequency and temperature; **a** Frequency dependence for several temperatures, **b** Temperature dependence for several frequencies

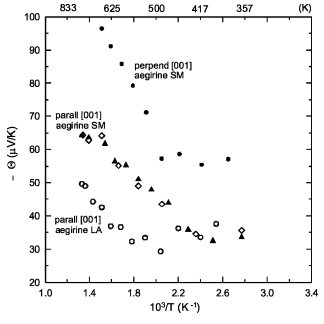

Fig. 10 Thermopower Θ as a function of the inverse of temperature for aegirine SM measured ∥ [001] and ⊥ [001] and for aegirine LA ∥ [001]

aegirine SM encompass two measurement runs in order to show the accuracy of measurement. It appears that a constant Θ exists in a certain temperature interval, but unfortunately this finding cannot be proved towards lower temperatures. At higher temperatures, the data can be described by the relation

$$\Theta = (k_B/|e|)(E_\Theta/k_B T + A) \ , \qquad (5)$$

where e is the elementary charge, E_Θ is the thermopower activation energy and A′ is a constant. Such a formula is predicted for small polaron hopping between localized states (Mott and Davis 1979). For small polaron hopping, in the activation energy E_Θ of Eq. (5) the term E_H, due to polarization, should not appear (Austin and Mott 1969). Thus, a difference from the activation energy of σ_{DC} can be considered as proof for the existence of small polarons.

For aegirine SM we found for data recorded ∥ [001] the activation energy $E_\Theta = 0.031$ eV and a constant $A^* = -1.24$, which contributes $\sim -107\ \mu V\ K^{-1}$ to Θ ($k_B/|e| = 86.2\ \mu V\ K^{-1}$); for measurements ⊥ [001] it follows that $E_\Theta = 0.071$ eV and $A^* = -2.41$, which contributes $\sim -208\ \mu V\ K^{-1}$ to Θ. Data of aegirine LA recorded ∥ [001] are $E_\Theta = 0.032$ eV and $A^* = -1.05$. This means that no essential difference exists between both aegirines for measurements ∥ [001]. The results for the activation energies E_Θ are within the range observed on amorphous semiconductors such as V_2O_5 gels (Sanchez et al. 1982) and Zn–Te–V oxide glasses (Singh and Chakravarthi 1997); very similar E_Θ values were established on disordered semiconductors such as Li-spinel ferrite (Whall et al. 1986), $La_2NiO_{4+\delta}$ (Demourges et al. 1996) and on various Mn-containing perovskite-type compounds in the semiconducting phase above the magnetic order temperature (Jaime et al. 1996; Hundley and Neumeier 1997; Niesbieskikwiat and Sanchez 2000). In all cases, the contribution to Θ by the constant A* is of the same order of magnitude as that of the term $E_\Theta/k_B T$.

Discussion

DC conductivity

The results of DC conductivity σ_{DC} and of AC conductivity $\sigma'(\omega)$ (Fig. 4a,b) suggest a small polaron hopping transport of charge carriers between localized levels. This model was successfully applied to the conductivity behaviour of amorphous and disordered (doped) semiconductors as mentioned (Mott and Davis 1979; Long 1982, 1991; Elliot 1987). The temperature dependence of the conductivity is provided by the thermally activated drift mobility of charge carriers, while their concentration remains fixed in contrast to band conduction. From the relation $\sigma = e\ n\ \langle\mu_D\rangle$ (n = concentration of charge carriers, $\langle\mu_D\rangle$ = mean drift mobility) it follows, for example at 500 K, from σ_{DC} data a value of $\langle\mu_D\rangle \sim 10^{-6}\ cm^2\ (Vs)^{-1}$. For hopping processes it is predicted $\langle\mu_D\rangle \ll 1\ cm^2\ (Vs)^{-1}$ (Austin

and Mott 1969); hence, in our situation the condition is amply satisfied at any measuring temperature. Application of Eq. (1) requires non-adiabatic hopping of small polarons. This means that the hopping probability of polarons during phonon excitation is small (Austin and Mott 1969).

Hopping of the type $Fe^{2+} \rightarrow Fe^{3+}$ can preferentially occur along zig-zag chains ∥ [001] in the clinopyroxene lattice (Fig. 1). The cation separation M1–M1 = 3.19 Å in ideal aegirine (Ballet et al. 1989) is consistent with the comparatively high experimental hopping activation energies. Electron hopping $Fe^{2+} \rightarrow Fe^{3+}$ may not necessarily proceed across common edges but take place through orbitals of intervening oxygen anions, i.e. a quasi-1 D conduction may occur. No immediately obvious hopping path appears to exist for any direction ⊥ [001], as mentioned earlier. For this kind of electron transfer to occur, hopping has to proceed via M2 and/or T sites which may be empty or occupied by Fe ions. Alternatively, some kind of lattice defects may provide charge transfer.

Suggesting electron transfer between M1 sites alone, one would assume a rather narrow distribution of relaxation times when the concentration of impurities and, hence, also of Fe^{2+} is very reduced. Both curves in Fig. 4a,b show no major qualitative difference apart from a shift in magnitude of the conductivity by a factor of 2–10. It is tempting to use as theoretical description of the experimental data the models of bundles of chains developed by the above authors, where charge hopping is dominant, but which allows interchain hopping of charges. In aegirine such an interpretation would be able to explain the notable conductivity ⊥ [001]. The average lengths of our octahedral chains ∥ [001] may be limited by defects.

AC conductivity

The experimental frequency dependence of $\sigma'(\omega)$ documents that the aegirines under study represent disordered semiconductors. The dispersion of $\sigma'(\omega)$ is indicative of a hopping charge-transport mechanism which is frequently characterized by a distribution of hopping relaxation times, originating from a distribution of energy barriers (Dyre 1988b). In nearly ideal aegirine, one would expect well-defined environments in terms of $Fe^{2+} \rightarrow Fe^{3+}$ hopping with a very low concentration of Fe^{2+} from M1 site to M1 site along zig-zag chains in the [001] direction; hence, rather homogeneous energy barriers for hopping processes are expected. One reason for the existence of disorder are Ca^{2+} (1.26 Å) introduced at the place of Na^{+} (1.32 Å). In particular for aegirine LA the concentration of Ca^{2+} (as well as that of Fe^{2+}) is comparably high, as found by Mössbauer spectroscopy. On the other hand, a clear dispersion of $\sigma'(\omega)$ is also found for aegirine SM with a much lower concentration of Ca^{2+} and, hence, of Fe^{2+}, although it is somewhat reduced relative to aegirine LA (Fig. 4). Disorder is also sensed by magnetic parameters. In natural aegirine with impurities, a distribution of magnetic exchange interactions between Fe ions, as established by Mössbauer analysis, was attributed to these impurities (Ballet et al. 1989).

Frequency dependence of AC conductivity

Theoretically, for Eq. (3) $\sigma(\omega) = [\sigma'(\omega) - \sigma_{DC}] \propto \omega^{s(T)}$, suggesting that σ_{DC} arises from a charge transport mechanism differing completely from that for $\sigma'(\omega)$. However, in our model it is presumed that $\sigma_{DC} = \lim_{\omega \rightarrow 0} \sigma'(\omega)$. In such a situation $\sigma'(\omega)$ is the adequate parameter in Eq. (3) (Emin and Ngai 1983). Equation (3) should hold, for instance, if there is a distribution of hopping relaxation times. At zero frequency, i.e. for DC charge transport, the charge carriers have to find a so-called percolation path for hopping from electrode to electrode, overcoming a large number of energy barriers of variable height in disordered semiconductors. For AC processes, the hopping paths back and forth in a cluster during a cycle for $\sigma'(\omega)$ decrease more and more in distance with increase in frequency. For the largest available frequency, a charge carrier is hopping only a short distance, possibly only to the next neighbour (pair hopping). In this situation a comparatively small activation energy is required and $\sigma'(\omega)$ is enhanced relative to σ_{DC}. The related processes are marked at low temperatures. Equation (3) was applied for the analysis of AC conductivity of iron-bearing trioctahedral phyllosilicates (Rüscher and Gall 1995).

The observed frequency variation of $\sigma'(\omega)$ excludes a charge transport mechanism from a localized level to an empty conduction band because no frequency dependence of $\sigma'(\omega)$ is expected in this case as mentioned. Figure 11 displays the temperature dependence of the exponent s (Eq. 3) in the linear portion of the curves for aegirine SM, measured ∥ and ⊥ [001]. Although values of s are subjected to an enhanced error, it can be seen that there is a marked difference between both directions for about the same temperature range. While ∥ [001], a limiting value of the exponent of $s \sim 1$, is reached at lower temperatures, only half of this magnitude is established ⊥ [001]. Hence, it appears that a difference in the distribution of hopping relaxation times exists. This fact may be related primarily to the different hopping paths ⊥ [001] relative to those ∥ [001].

AC conduction models of hopping charge transport were applied to oxide glasses where transition metal ion couples such as Fe^{2+}–Fe^{3+} or V^{4+}–V^{5+} are responsible for hopping conduction (Gosh 1990, 1993). Various of these models of charge transport were applied to the conductivity of a series of disordered oxidic mixed crystal semiconductors and found to be realized (Chen et al. 1989, 1991; Samara et al. 1990; Zuppiroli et al. 1991; Singh et al. 1996; Jhans et al. 1996). Disorder is here evidently caused by a variation in ion sizes and charges for fixed lattice sites which gives rise to a

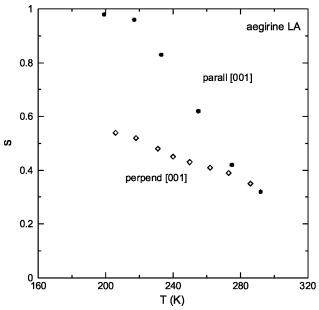

Fig. 11 Variation of the exponent s with temperature for aegirine LA, measured ∥ [001] and ⊥ [001]

variation of spatial environments for sites involved in hopping as in our aegirines.

Because of the limited T range, a quantitative verification of theoretical hopping models is made difficult. It seems that the exponent $s < 1$ in both crystallographic directions. Measurements ∥ [001] show a strong temperature variation while it is reduced ⊥ [001]. A temperature dependence of the exponent s is theoretically predicted for: (1) correlated over barrier hopping and (2) large polaron hopping in the tunnelling regime.

Scaling law of AC conductivity

There is in fact a single curve with weak deviations of data points; only those were taken into account which refer to the bulk arc 1 in Fig. 3. It seems as if the EPA model may be applicable to hopping conduction processes in aegirine at least in the temperature range < 300 K. A similar scaling curve is established for aegirine SM. The above function $F(x)$ describes the data points adequately only for not too high values of the normalized frequency. Such a master curve by scaling was observed on a variety of disordered semiconductors as, for instance, on Mn–Co–Ni–Cu spinels (Suzuki 1980), polyacetylene (Summerfield 1985), *n*-InSb (Abboudy et al. 1988), porous Si (Ben-Chorin et al. 1995), $La_2NiO_{4+\delta}$ (Jhans et al. 1996), and carbon black (Brom et al. 1998).

AC losses

Frequently peaks are found for dielectrics if loss mechanisms are acting in the form of electric dipoles with the loss peak at frequency ω_m which coincides with the relaxation frequency ω_0 of the orientable dipoles. For hopping-type charge transport, loss peaks are expected close to frequencies, where $\sigma'(\omega)$ begins to rise above σ_{DC} with increase in frequency. In the low-frequency range, a critical frequency $\omega_c(T)$ is thought to exist with $\sigma_{DC} \sim \sigma(\omega_c)$, while for $\omega > \omega_c$ the conductivity $\sigma'(\omega)$ begins to rise. The loss peak frequency ω_m is close to ω_c (Dyre 1988a). As $\omega < \omega_c$ is the frequency range where hopping electrons can percolate from electrode to electrode, ω_c may mark the onset of hopping in clusters of variable lengths which represent the low-frequency limit of the applicability of the pair approximation (Hunt 1991b, 1993). As mentioned above, hopping between pairs of sites can be considered as rotating dipoles with a relaxation frequency, related to loss peaks.

For temperatures 223, 247 and 270 K, a nearly linear fall off of $\varepsilon''(\omega)$ is established for increasing frequencies; eventually, at 270 K in the region of the lowest frequencies an onset to a peak may occur. Earlier, such behaviour was considered as anomalous low-frequency dispersion of a dielectric (Jonscher 1978). The data may represent high-frequency flanks of loss peaks. In the frequency regime of a strict power law $\sigma'(\omega) \propto \omega^s$ it follows that $\varepsilon''(\omega) \propto \omega^{-m}$ with $m = 1 - s$. In our case of an approximate power law for $\sigma'(\omega)$ at rather high-frequencies, we observe from Fig. 8a a fairly satisfying power law for $\varepsilon''(\omega)$ in a medium to low-frequency range at all four temperatures; at 270 K we deduce from a fit of the steepest slope $m = 0.95$. If we separate formally our $\sigma'(\omega)$ into two categories of hopping processes, one due to processes which enable percolation from electrode to electrode (giving rise to σ_{DC}) and all the others related to clusters of variable sizes with approximately $\sigma_C(\omega) \propto A\omega^s$, then we may write $\sigma'(\omega) = \sigma_{DC} + \sigma_C(\omega)$; from $\varepsilon''(\omega) \propto \sigma_{DC}/\varepsilon_0\omega + \sigma_C(\omega)/\varepsilon_0\omega$ it follows that if the second term would not contribute, it would result a slope $m = 1$. If $m = 0.95$, the slope is largely dictated by the contribution of σ_{DC}. At the lowest frequencies, there is only a weak deviation from a straight line (with the exception at 270 K) which corresponds in the Z'–Z'' diagram to frequencies which lie on the arc 2 (Fig. 3). Quite analogous curves as in Fig. 8a were observed on $Sr(Fe_{1-x}Nb_x)O_{2.5+\gamma}$ perovskites (Liu et al. 1993), on chain polymers (Cappacioli et al. 1998) and on V-phosphate glasses doped with Li (Salman et al. 2002). For some glasses, loss plots $\log \varepsilon''(\omega) - \log \omega$ showed peaks only after σ_{DC} was subtracted from $\sigma'(\omega)$ (Dyre 1988a).

Dielectric permittivity

The dielectric permittivity is composed of several contributions $\varepsilon'(\omega) = \varepsilon_\infty(\omega) + \varepsilon_l(\omega) + \varepsilon_d(\omega)$;$\varepsilon_\infty(\omega)$ is the high-frequency dielectric permittivity which is due to electronic displacements inside ions, $\varepsilon_l(\omega)$ is the contribution to the permittivity caused by elastic displacement of ions in the lattice, $\varepsilon_d(\omega)$ is due to dipolar polarization which arises from permanent dipoles and effects which can be described in terms of the picture of orientable dipoles such as pair hopping of electrons between two localized levels as mentioned (Fröhlich 1958; Samara et al. 1990). In the region of large variation at high temperatures (Fig. 9a), hopping is enhanced and $\varepsilon'(\omega)$ is dominated by $\varepsilon_d(\omega)$; at low temperatures with considerable reduction in hopping and weak dispersion $\varepsilon_l(\omega) + \varepsilon_d(\omega)$ appear to be the major contributions to $\varepsilon'(\omega)$. There is no saturation towards the static

$\varepsilon'(0) = \lim_{\omega \to 0} \varepsilon'(\omega)$, since a steep rise in $\varepsilon'(\omega)$ in this region for $\omega \to 0$ (Fig. 9a) is probably dictated by electrode contact effects which are reflected by arc 2 in Fig. 3. No anomaly is evident from either figure which would point to still unknown effects. Quite a similar dispersion of $\varepsilon'(\omega)$ was observed on the insulating tetragonal phase of $YBa_2Cu_3O_{6+x}$ ($x \sim 0$) (Samara et al. 1990) and on La_2CuO_{4+y} in the insulating state (Chen et al. 1989).

Thermopower

In disordered semiconductors, in which conduction takes place by small polaron hopping with a fixed concentration of charge carriers, Θ is frequently constant at higher temperatures when a single kind of charge carriers exists (Tuller and Nowick 1977; Srinivasan and Srivastava 1981). The negative Θ is compatible with the picture of electron hopping $Fe^{2+} \rightarrow Fe^{3+}$. Here, Fe^{2+} ions act as donors as mentioned earlier.

If $k_B/T > E_D$, a formula may be applied describing approximately Θ for mixed valence charge transport of small polarons with

$$\Theta = (k_B/|e|)[E_H/20k_BT + S_0] \ , \qquad (6)$$

where S_0 is a constant consisting of two contributions $S_0 = S_1 + S_2$; E_H is the hopping activation energy, due to polarization, as defined earlier and e the electronic charge. $E_H/20$ corresponds to E_Θ in Eq. (5) and the second term S_0 to the constant A′. $S_1 = \ln [c/(1-c)]$ where c is the ratio of the number of charge carriers to hopping sites as defined above (the expression is subject to the constraint that no site is doubly occupied) and the formula applies to 1 D conduction. The spin degeneracy term $S_2 = \ln[(2I_n + 1)/(2I_{n+1} + 1)]$, where for a couple of mixed valence cations M^{n+} and $M^{(n+1)+}$ the quantity I_n = spin value of the cation M^{n+} and I_{n+1} = spin value of the cation $M^{(n+1)+}$; in our case of suggested $Fe^{2+} \rightarrow Fe^{3+}$ electron hopping ($I_n = 2$ for Fe^{2+} and $I_{n+1} = 5/2$ for Fe^{3+}) it results $S_2 = \ln(5/6)$ (Heikes et al. 1963; Austin and Mott 1969; Yoo and Tuller 1988; Doumerc 1994). For $1/T \rightarrow 0$, Eq. (6) with $S_0 = S_1$ is referred to as the Heikes formula. For high temperatures, variations of the Heikes formula were theoretically derived, depending on the kind of interactions (Chaikin and Beni 1976). For magnetic semiconductors there is an additional term in the bracket which is for T above the magnetic order temperature T_c given by $S_{mag} = -\gamma J^2/k_B^2T^2$; J is the exchange integral between adjacent spins with $k_BT_c = 2J$, $\gamma = 5/3$ and 5 for 1 D and 3 D models, respectively (Liu and Emin 1984). For aegirine with Fe^{2+} and Fe^{3+}, it follows from the spin degeneracy term a constant contribution to the thermopower of $\Theta_{spin} = -15.7\ \mu VK^{-1}$; the temperature-dependent magnetic contribution can be ignored in view of the low Néel temperature $T_N \sim 10$ K of aegirine (Ballet et al. 1989). When the force constants of the ions for the pair of hopping sites are different and the activation energy is not equally divided between both sites, a term (E_H/k_BT) $(1 - \varphi)/(1 + \varphi)$ arises where φ is the ratio of force constants, which results in approximately $E_H/20k_BT$ (Austin and Mott 1969).

Suppose for aegirine SM for instance $c = 0.02$. It follows for the contribution of the first term to Θ in Eq. (6) at 700 K with the experimental $E_H \sim 0.43$ eV, extracted from σ_{DC} data, a value of $\sim +\ 31\ \mu VK^{-1}$, and for lower temperatures the magnitude is enhanced. The second term gives a value of $\sim -\ 336\ \mu VK^{-1}$. On the other hand, taking the measured $E_\Theta = 0.031$ eV, it follows from Eq. (6) that $E_H = 0.62$ eV, considerably above 0.43 eV. In both cases, the correct trend for the variation of Θ with T is met, although not the proper magnitude. In order to come to a reasonable result, approximately describing the experimental data, it is required $c \sim 0.25$, which implies a much higher concentration of charge carriers. Such a magnitude could be achieved if only part of all Fe^{3+} are available as hopping sites for electrons jumping from Fe^{2+} to Fe^{3+} ions. In this picture possibly constant Θ for $T \leq 400$ K can hardly be explained. An analogous reasoning can be made for data recorded on aegirine LA.

The localized levels of the Fe^{2+}/Fe^{3+} couples on the energy scale have doubtless to be placed between the low lying $2p$ oxygen valence band and the empty $4s$ Fe conduction band. The spread in energy of the levels is given by the experimental $E_D < 0.1$ eV, provided all Fe ions take part in conduction $\parallel$ as well as $\perp$ [001]. Otherwise, this value may refer only to a group of Fe^{2+}/Fe^{3+} which are involved in charge transport.

We have in principle to look for any lattice defects in our aegirine crystals, as they can contribute to conduction. At the moment we have no information of possible cation vacancies on M1 and M2 sites which may act as donors or acceptors. Possibly nano-scale exsolution of other silicate phases may represent obstacles, affecting hopping conduction to a variable degree. Such defects were detected in jadeite ($NaAlSi_2O_6$) (Wu et al. 2002). Whether exsolution on an atomic scale is possible in aegirine and what effect it may exert on electrical conduction, does not appear to be known yet. Such a situation may give rise to a large variation in hopping paths related to a broad variation in energy barriers.

Summary and conclusions

DC and AC conductivity measurements (20 Hz–1 MHz) on two aegirines, measured $\parallel$ and $\perp$ to the [001] direction, showed a semiconducting behaviour with a strong dispersion of AC data at lower temperatures, which is indicative of a hopping-type charge conduction of small polarons. The DC conductivity is described by the model of small polaron hopping in the whole temperature range between ~200 and 600 K. Below room temperature, DC data can also be approximated using the concept of variable range hopping. There is an anisotropic behaviour with enhanced conduction along [001]. The experimental

frequency dependence of the AC conductivity with a power law is also typical for charge transport by small polarons. The assumption that Fe^{2+} ions, present in low concentrations, act as donors for conduction of the kind $Fe^{2+} \rightarrow Fe^{3+}$ at least for measurements $\parallel$ [001], is consistent with the determined drift mobility $\mu_D << 1\ cm^2(Vs)^{-1}$, which is characteristic for hopping charge transport. The property of scaling of the DC and AC conductivities documents that both are related to the same hopping charge transport mechanism. In terms of $Fe^{2+} \rightarrow Fe^{3+}$ electron hopping, transport paths along zig-zag chains $\parallel$ [001] are immediately evident from the pyroxene structure, while $\perp$ [001] such paths are only possible via intervening M2 and/or T sites as well as via impurities and vacancies.

Thermopower data recorded $\parallel$ and $\perp$ [001] between 350 and 770 K are compatible with assumed small polaron hopping of the kind $Fe^{2+} \rightarrow Fe^{3+}$. Above ~400 K, the strong temperature dependence of the thermopower is tentatively described in terms of a formula developed for mixed valence semiconductors with hopping-type conduction.

Acknowledgements The authors are indebted to the Deutsche Forschungsgemeinschaft for financial support. The positive criticism and helpful suggestions by two reviewers are gratefully acknowledged.

References

Abboudy S, Fozooni P, Mansfield R, Lea MJ (1988) Finite frequency scaling of hopping conductivity in *n*-InSb. Phil Mag Lett 57: 277–282

Amthauer G, Rossman GR (1984) Mixed valence of iron in minerals with cation clusters. Phys Chem Miner 11: 37–51

Austin IG, Mott NF (1969) Polarons in crystalline and non-crystalline materials. Adv Phys 18: 41–102

Ballet O, Coey JMD, Fillion G, Ghose A, Hewat A, Regnard JR (1989) Magnetic order in aegirine; $NaFeSi_2O_6$. Phys Chem Miner 16: 672–677

Ben-Chorin M, Möller F, Koch F, Schirmacher W, Eberhard M (1995) Hopping transport on a fractal: AC conductivity of porous silicon. Phys Rev 51: 2199–2213

Bleibaum O, Böttger H, Bryksin VV (1996) Effective medium theory of hopping transport. Phys Rev (B) 54: 5444–5452

Bloch AN, Weisman RB, Varma CM (1972) Identification of a class of disordered one-dimensional conductors. Phys Rev Lett 28: 753–756

Brenig W, Döhler GH, Heyszenau H (1973) Hopping conductivity in highly anisotropic systems. Phil Mag 27: 1093–1103

Brom HB, Reedijk JA, Martens HCF, Adriaanse LJ, de Jongh LJ, Michels MAJ (1998) Frequency and temperature scaling in the conductivity and its structural consequences. Phys Stat Sol (b) 205: 103–108

Buseck PR, Nord GL, Jr, Veblen DR (1980) In: Prewitt CD (ed.) Reviews in mineralogy, vol 7: pyroxenes. Mineralogical Society of America, Washington, DC, p. 117

Cameron M, Papike JJ (1981) Structural and chemical variations in pyroxenes. Am Mineral 66: 1–50

Capaccioli S, Lucchesi M, Rolla PA, Ruggeri G (1998) Dielectric response analysis of a conducting polymer dominated by the hopping charge transport. J Phys: Condens Matter 10: 5595–5617

Chaikin PM, Beni G (1976) Thermopower in the correlated hopping regime. Phys Rev 13: 647–651

Chen CY, Preyer NW, Picone PJ, Kastner MA, Jenssen HP, Gabbe DR, Cassanho A, Birgeneau RJ (1989) Frequency dependence of the conductivity and dielectric constant of La_2CuO_{4+y} near the insulator-metal transition. Phys Rev Lett 63: 2307–2310

Chen CY, Birgeneau RJ, Kastner MA, Preyer NW, Thio T (1991) Frequency and magnetic-field-dependence of the dielectric constant and conductivity of $La_2CuO_{4+\gamma}$. Phys Rev (B) 43: 392–401

Demourges A, Dordor P, Doumerc J-P, Grenier J-C, Marquestaut E, Pouchard M, Villesuzann A, Wattiaux A (1996) Transport and magnetic properties of $La_2NiO_{4+\delta}$ ($0 \le \delta \le 0.25$). J Solid State Chem 12: 199–204

Dollase WA, Gustafson WI (1982) ^{57}Fe Mössbauer spectral analysis of the sodic clinopyroxenes. Am Mineral 67: 311–327

Doumerc J-P (1994) Thermoelectric power for carriers in localized states: a generalization of Heikes and Chaikin-Beni formulae. J Solid State Chem 109: 419–420

Dyre JC (1988a) The random free-energy barrier model for AC conduction in disordered solids. J Appl Phys 64: 2456–2468

Dyre JC (1988b) Some remarks on AC conduction in disordered solids. J Non-Crystalline Solids 135: 219–226

Efros AL, Shklovskii BI (1975) Coulomb gap and low temperature conductivity of disordered systems. J Phys (C): Solid State Phys 8: L49–L51

Elliot SR (1987) A.C. conduction in amorphous chalcogenide and pnictide semiconductors. Adv Phys 36: 135–218

Emin D, Ngai KL (1983) Hopping conduction in lightly doped polyacetylene. J Phys Coll C3 44: 471–475

Fröhlich H (1958) Theory of dielectrics. Oxford University Press, Oxford

Gosh A (1990) Frequency-dependent conductivity in bismuth-vanadate glasses. Phys Rev (B) 41: 1479–1488

Gosh A (1992) Correlated-barrier hopping in semiconducting tellurium molybdate glass. Phys Rev (B) 45: 11318–11320

Gosh A (1993) Complex AC conductivity of tellurium cuprate glassy semiconductors. Phys Rev (B) 47: 15537–15542

Heikes RR, Maradudin AA, Miller RC (1963) Une étude des propriétés de transport des semiconducteurs de valence mixte. Ann Phys 8: 733–746

Huebner JS, Duba A, Wiggins LG (1979) Electrical conductivity of pyroxene which contains trivalent cations: laboratory measurements and the lunar temperature profile. J Geophys Res 84: 4652–4656

Hundley MF, Neumeier JJ (1997) Thermoelectric power of $La_{1-x}Ca_xMnO_{3+\delta}$: inadequacy of the nominal Mn^{3+4+} valence approach. Phys Rev (B) 55: 11511–11515

Hunt A (1991a) One-dimensional hopping conductivity calculations. Phil Mag (B) 64: 327–334

Hunt A (1991b) The AC conductivity of the Fermi glass: a model for glassy conduction. Solid State Commun 80: 151–155

Hunt A (1993) A general treatment of one-dimensional hopping conduction. Solid State Commun 86:765–768

Jonscher AK (1978) Low-frequency dispersion in carrier-dominated dielectrics. Phil Mag (B) 38: 587–601

Jaime M, Salamon MB, Rubinstein M, Treece RE, Horwitz JS, Chrisey DB (1996) High-temperature thermopower in $La_{2/3}Ca_{1/3}MnO_3$ films: evidence for polaronic transport. Phys Rev (B) 54: 11914–11917

Jhans H, Kim D, Rasmussen RJ, Honig JM (1996) AC-conductivity measurements on $La_2NiO_{4+\delta}$. Phys Rev (B) 16: 11224–11229

Koscielska B, Murawski L, Chudinov S, Stizza S (1999) Hopping conduction in glassy and crystallized Bi–Sr–Ca–Cu–O system. Phys Stat Sol (B) 211: 751–757

Liu N-L, Emin D (1984) Thermoelectric power of small polarons in magnetic semiconductors. Phys Rev 30: 3250–3256

Liu D, Yao X, Smyth DM, Bhalla AS, Cross LE (1993) Structure order–disorder and dielectric response in perovskite-related $SrO–Fe_2O_3–Nb_2O_5$ system: the oxygen-deficient composition $Sr(Fe_{1-x}Nb_x)O_{2.5+\gamma}$ ($x = 0.17,\ 0.25,\ 0.50$). J Appl Phys 74: 3345–3356

Long AR (1982) Frequency-dependent loss in amorphous semiconductors. Adv Phys 31: 553–637

Long AR (1991) Hopping conductivity in the intermediate frequency regime. In: Pollak M, Shklovskii B (eds.) Hopping transport in solids. Elsevier, Amsterdam, pp 207–231

Long AR, McMillan J, Balkan N, Summerfield S (1988) The application of the extended pair approximation to hopping conduction in r.f. sputtered amorphous silicon. Phil Mag (B) 58: 153–169

Moore JP, Graves RS (1973) Absolute Seebeck coefficient of platinum from 80 to 340 K and the thermal and electrical conductivities of lead from 80 to 400 K. J Appl Phys 44: 1174–1178

Mott NF (1968) Conduction in glasses containing transition metal ions. J Non-Crystalline Solids 1: 1–17

Mott NF, Davis EA (1979) Electronic processes in non-crystalline materials. Clarendon, Oxford

Niebieskikwiat D, Sanchez RD (2000) Correlation between thermoelectric properties and magnetic phases in the charge-ordered $Pr_{0.5}Sr_{0.5-x}Ca_xMnO_3$. J Magn Magn Mat 221: 285–292

Nolan J (1969) Physical properties of synthetic and natural pyroxenes in the system diopside–hedenbergite–aegirine. Miner Mag 37: 216–229

Parkhomenko EI (1982) Electrical resistivity of minerals and rocks at high temperature and pressure. Rev Geophys Space Phys 20: 193–218

Parkhomenko EI, Mkrtchian SA (1974) Chemical composition as the determining factor of electrical conductivity of minerals at high pressures (1–20 kbar) and temperatures (200–650 °C). Izv Akad Nauk SSSR Earth Phys 12: 46–58

Redhammer GJ, Amthauer G, Lottermoser W, Treutmann W (2000) Synthesis and structural properties of clinopyroxenes of the hedenbergite $CaFe^{2+}Si_2O_6$ -aegirine $NaFe^{3+}Si_2O_6$ solid-solution series. Eur J Mineral 12: 105–120

Rüscher CH, Gall S (1995) On the polaron-mechanism in iron-bearing trioctahedral phyllosilicates: an investigation of the electrical and optical properties. Phys Chem Miner 22: 468–478

Salman F, Shash N, Mohammed S, El-Mansy M (2002) Electrical conduction and dielectric properties of vanadium phosphate glasses doped with lithium. J Phys Chem Solids 63: 1957–1966

Samara GA, Hammeter WF, Venturini EL (1990) Temperature and frequency dependencies of the dielectric properties of $YBa_2Cu_3O_{6+x}$ ($x \sim 0$). Phys Rev (B) 41: 8974–8980

Sanchez C, Babonneau F, Morineau R, Livage J, Bullot J (1982) Semiconducting properties of V_2O_5 gels. Phil Mag (B) 47: 279–290

Sayer M, Mansingh A, Reyes JM, Rosenblatt G (1971) Polaronic hopping conduction in vanadium phosphate glasses. J Appl Phys 42: 2857–2864

Schmidbauer E, Kunzmann T, Fehr T, Hochleitner R (2000) Electrical resistivity and ^{57}Fe Mössbauer spectra of Fe-bearing calcic amphiboles. Phys Chem Miner 27: 347–356

Schnakenberg J (1968) Polaronic impurity hopping conduction. Phys Stat Sol 28: 623–633

Sen S, Gosh A (1999) Multiphonon assisted hopping in strontium vanadate semiconducting glasses. J Phys: Condens Matter 11: 1529–1536

Serota RA, Kalia RK, Lee PA (1986) New aspects of variable-range hopping in finite one- dimensional wires. Phys Rev (B) 33: 8441–8446

Shante VKS, Varma CM, Bloch AN (1973) Hopping conductivity in "one-dimensional" disordered compounds. Phys Rev (B) 8: 4885–4889

Singh R, Chakravarthi JS (1997) DC conductivity of V_2O_5-containing zinc tellurite glasses. Phys Rev (B) 55: 5550–5553

Singh R, Narula AK, Tandon RP, Mansingh A, Chandra S (1996) Low-frequency alternating current conduction and dielectric relaxation in polypyrrole, poly(N-methyl pyrrole), and their copolymers. J Appl Phys 80: 985–992

Srinivasan G, Srivastava CM (1981) Electrical conductivity mechanism in zinc and copper substituted magnetite. Phys Stat Sol (B) 103: 665–671

Summerfield S (1985) Universal low-frequency behaviour in the A.C. hopping conductivity of disordered systems. Phil Mag (B) 52: 9–22

Suzuki M (1980) A.C. hopping conduction in Mn–Co–Ni–Cu complex oxide semiconductors with spinel structure. J Phys Chem Solids 41: 1253–1260

Tsai YT, Whitmore DH (1982) Non-linear least-squares analyses of complex impedance and admittance data for solid electrolytes. Solid States Ionics 7: 129–139

Tuller HL, Nowick AS (1977) Small polaron electron transport in reduced CeO_2 single crystals. J Phys Chem Solids 38: 859–867

Van Staveren MPI, Brom HB, De Jongh LJ (1990) Metal-cluster compounds and universal features of the hopping conductivity of solids. Phys Rep 208: 1–96

Wang ZH, Ray A, MacDiarmid AG, Epstein AJ (1991) Electron localization and charge transport in poly(o-toluidine): a model polyaniline derivative. Phys Rev (B) 43: 4373–4384

Whall TE, Salerno N, Proykova Y, Mirza KA, Mazen S (1986) The electrical conductivity and thermoelectric power of lithium ferrite in the vicinity of the order–disorder transition temperature. Phil Mag 53: L107–L113

Wu X, Han Y, Meng D, Li D (2002) Discovery and implication of $P2_1/n$ crystal structure on a nano-scale in single jadeite crystals. Earth Planet Science Lett 197: 165–169

Yoo H-I, Tuller HL (1988) Analytic calculation of cation distributions in ferrite spinel $Mn_{1-\gamma}Fe_{2+\gamma}O_4$. J Phys Chem Solids 49: 761–766

Zuppiroli L, Papandreu N, Kormann R (1991) The dielectric response of boron carbide due to hopping conduction. J Appl Phys 70: 246–252